Cavity collapse near slot geometries: Supplementary Material

Elijah D. Andrews†[1], David Fernández Rivas[2] and Ivo R. Peters[1]

June 16, 2020

[1]Faculty of Engineering and Physical Sciences, University of Southampton, Southampton SO17 1BJ, UK
[2]Mesoscale Chemical Systems Group, MESA+ Institute, TechMed Centre and Faculty of Science and Technology, University of Twente, P.O. Box 217, 7500AE Enschede, The Netherlands

† Email address for correspondence: e.d.andrews@soton.ac.uk

1 All Comparison Plots

The figures presented here are comparison plots for all the experimental data listed in table 1, copied here from the paper. These plots show that the numerical predictions compare well to the experimental data. The numerical model tends to under-predict the peak jet angle, but the position of the peak jet angle is well predicted and the peak jet angle is typically close.

Label	W (mm)	H (mm)	Y values measured (mm)	h	y
W1H3	1.23	2.74	1.94, 2.91, 3.89	2.23	1.58, 2.37, 3.16
W2H3a	2.20	2.70	1.77, 2.29, 2.81, 3.32, 3.84	1.23	0.80, 1.04, 1.28, 1.51, 1.75
W2H3b	2.20	2.90	2.66, 3.68	1.32	1.21, 1.67
W2H6	2.20	5.40	1.52, 1.99	2.45	0.69, 0.90
W2H9	2.14	8.21	1.66, 2.66	3.84	0.78, 1.24
W2H12	2.20	11.50	2.63	5.23	1.20
W4H12	4.20	11.47	2.43, 3.43	2.73	0.58, 0.82

Table 1: Measurements of geometries used. Labels refer to the nominal width and height. This table is copied from the paper.

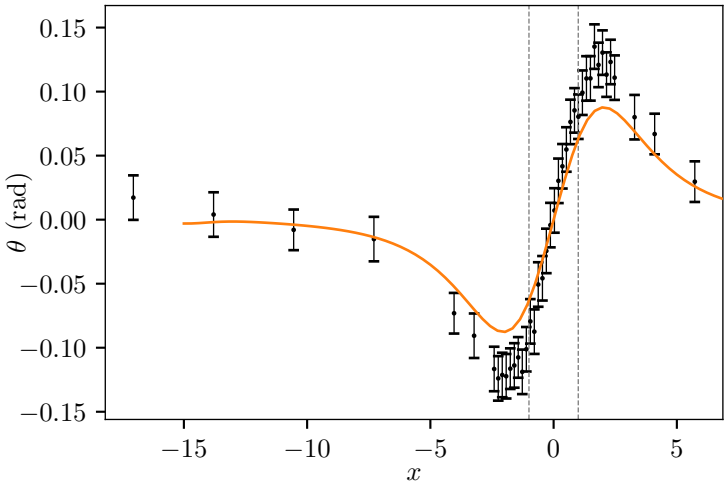

Figure 1: A comparison between experimental data (points with error bars) and a numerical prediction (solid line) for $W = 1.23$, $H = 2.74$, and $Y = 1.94$.

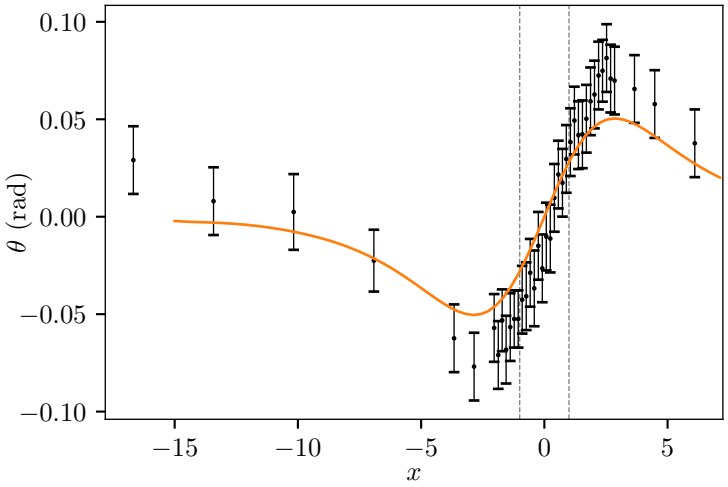

Figure 2: A comparison between experimental data (points with error bars) and a numerical prediction (solid line) for $W = 1.23$, $H = 2.74$, and $Y = 2.91$.

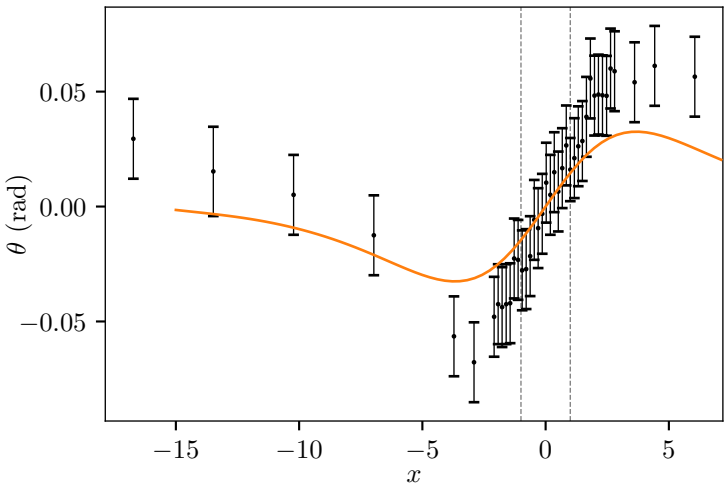

Figure 3: A comparison between experimental data (points with error bars) and a numerical prediction (solid line) for $W = 1.23$, $H = 2.74$, and $Y = 3.89$.

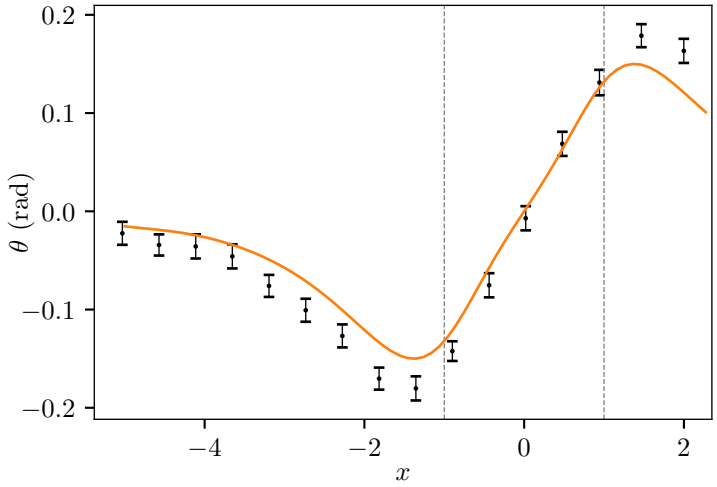

Figure 4: A comparison between experimental data (points with error bars) and a numerical prediction (solid line) for $W = 2.20$, $H = 2.70$, and $Y = 1.77$.

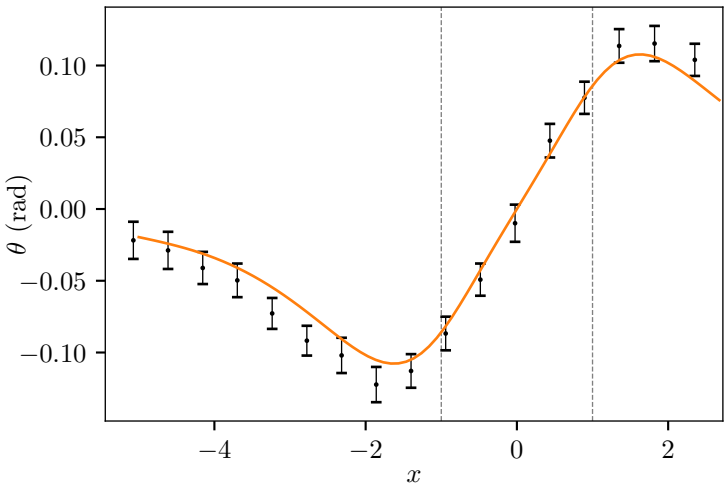

Figure 5: A comparison between experimental data (points with error bars) and a numerical prediction (solid line) for $W = 2.20$, $H = 2.70$, and $Y = 2.29$.

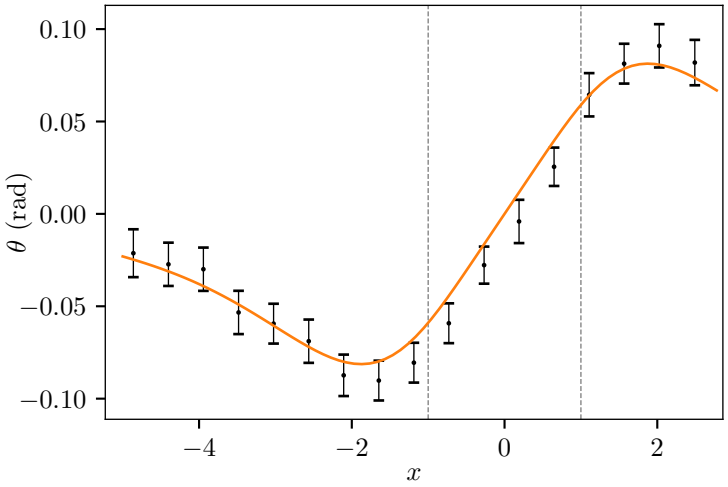

Figure 6: A comparison between experimental data (points with error bars) and a numerical prediction (solid line) for $W = 2.20$, $H = 2.70$, and $Y = 2.81$.

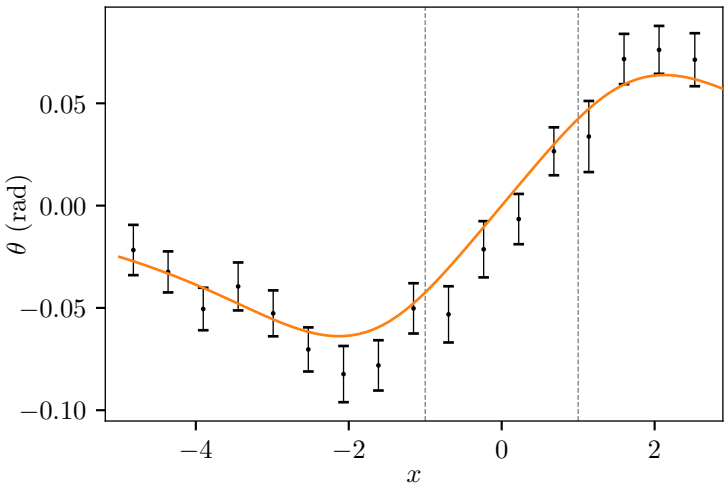

Figure 7: A comparison between experimental data (points with error bars) and a numerical prediction (solid line) for $W = 2.20$, $H = 2.70$, and $Y = 3.32$.

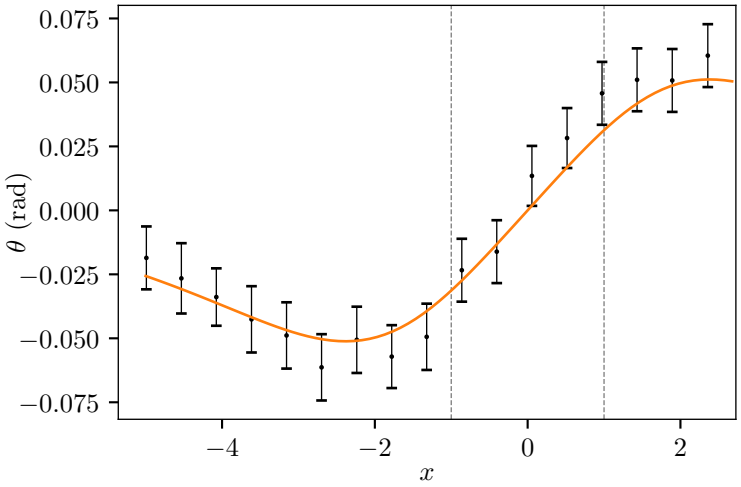

Figure 8: A comparison between experimental data (points with error bars) and a numerical prediction (solid line) for $W = 2.20$, $H = 2.70$, and $Y = 3.84$.

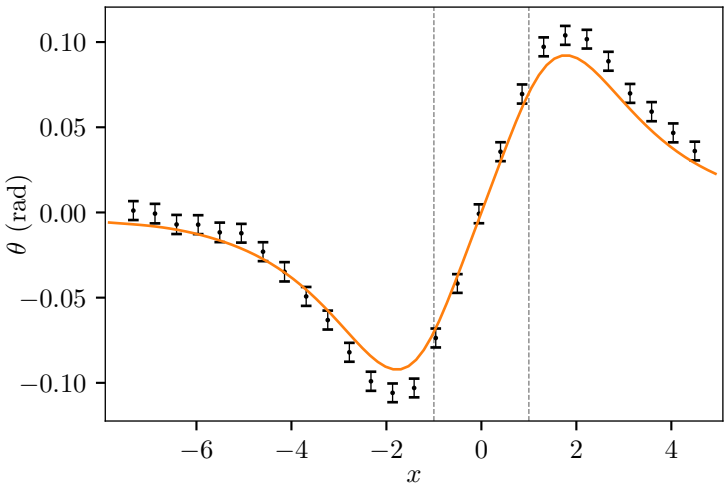

Figure 9: A comparison between experimental data (points with error bars) and a numerical prediction (solid line) for $W = 2.20$, $H = 2.90$, and $Y = 2.66$.

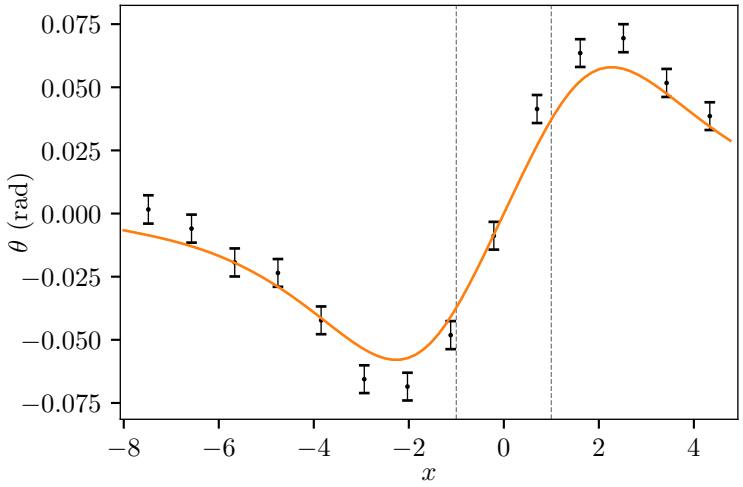

Figure 10: A comparison between experimental data (points with error bars) and a numerical prediction (solid line) for $W = 2.20$, $H = 2.90$, and $Y = 3.68$.

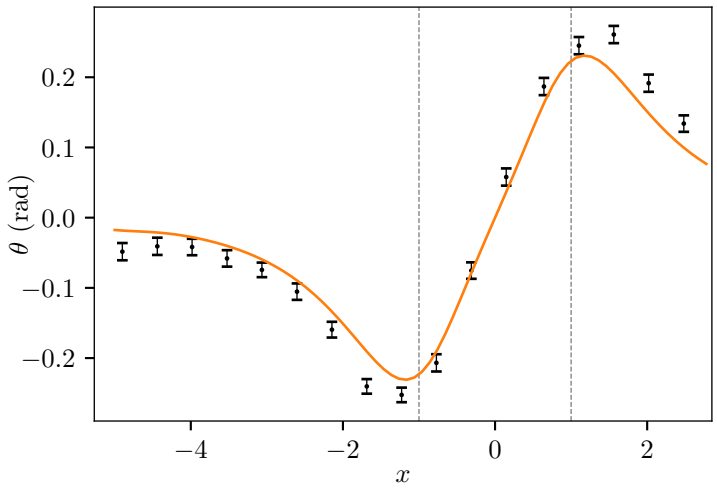

Figure 11: A comparison between experimental data (points with error bars) and a numerical prediction (solid line) for $W = 2.20$, $H = 5.40$, and $Y = 1.52$.

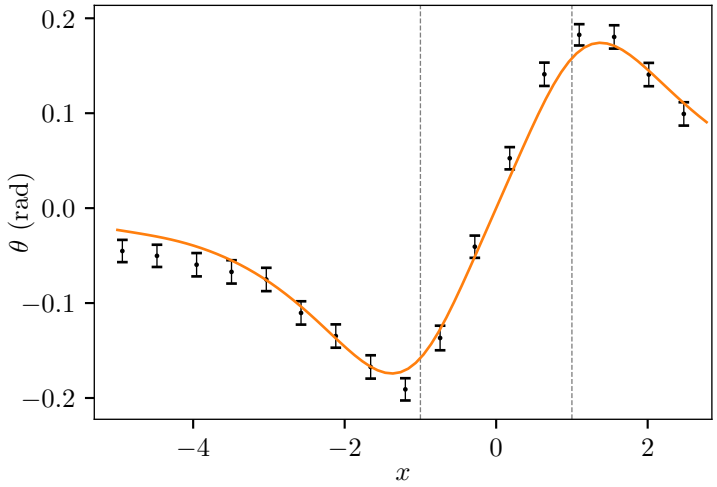

Figure 12: A comparison between experimental data (points with error bars) and a numerical prediction (solid line) for $W = 2.20$, $H = 5.40$, and $Y = 1.99$.

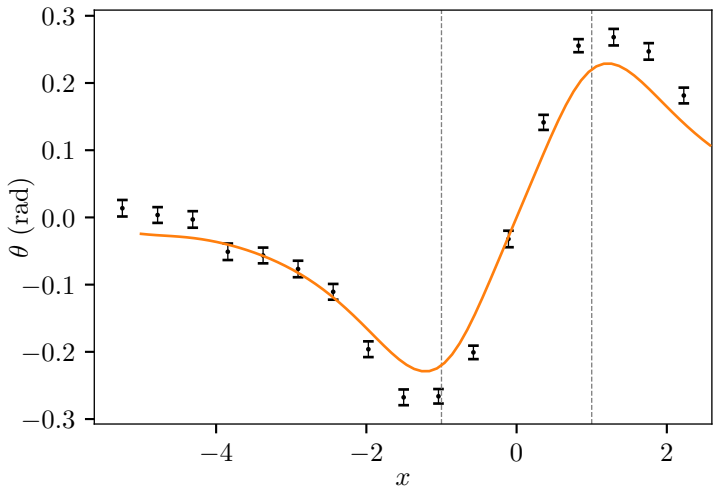

Figure 13: A comparison between experimental data (points with error bars) and a numerical prediction (solid line) for $W = 2.14$, $H = 8.21$, and $Y = 1.66$.

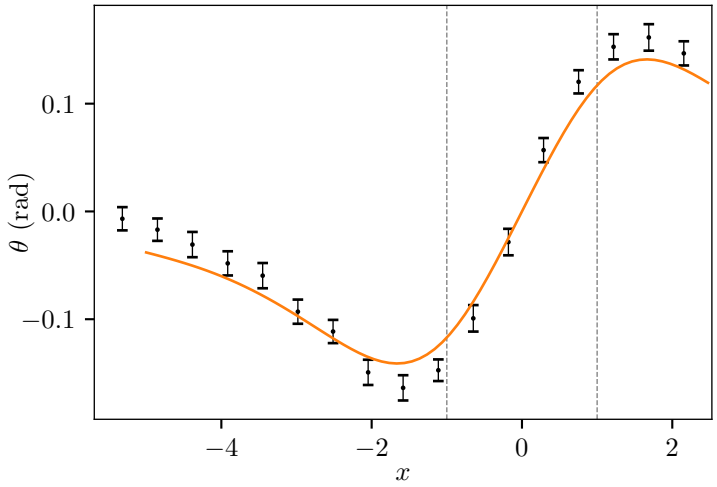

Figure 14: A comparison between experimental data (points with error bars) and a numerical prediction (solid line) for $W = 2.14$, $H = 8.21$, and $Y = 2.66$.

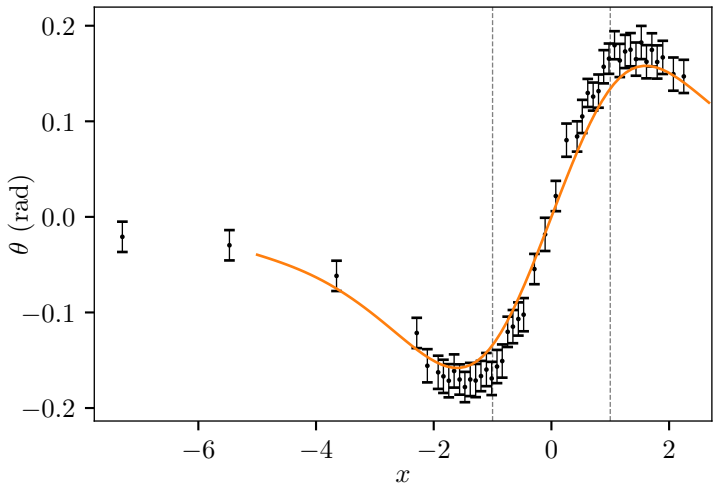

Figure 15: A comparison between experimental data (points with error bars) and a numerical prediction (solid line) for $W = 2.20$, $H = 11.50$, and $Y = 2.63$.

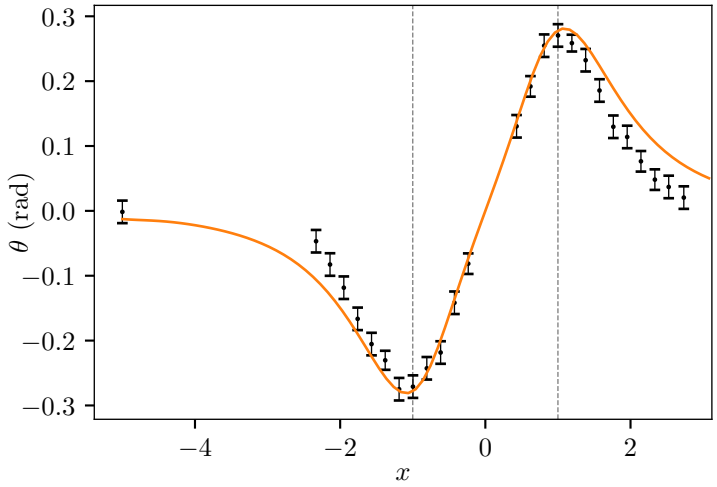

Figure 16: A comparison between experimental data (points with error bars) and a numerical prediction (solid line) for $W = 2.20$, $H = 11.47$, and $Y = 2.43$.

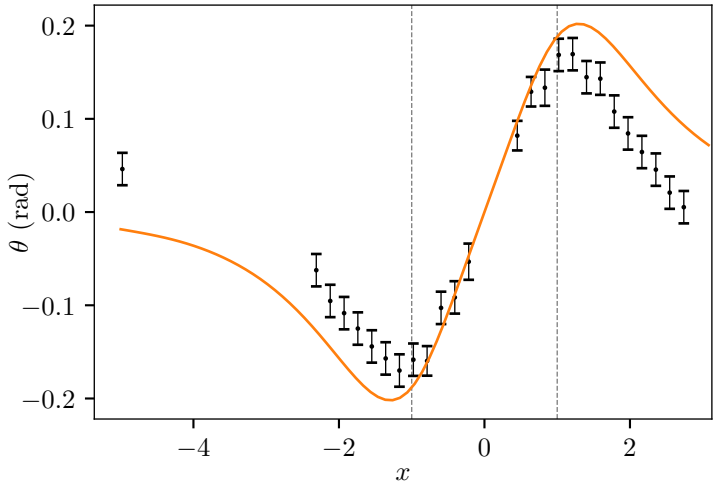

Figure 17: A comparison between experimental data (points with error bars) and a numerical prediction (solid line) for $W = 2.20$, $H = 11.47$, and $Y = 3.43$.

2 Dependence of jet angle variation on displacement

From analysis of the two sweeps for the W2H3b geometry, we do not observe any significant variation in jet deviation based on jet strength. Figures 18 and 19 in this material show the normalised jet angle deviation as a function of the normalised displacement, Δ/R, where Δ is the bubble displacement between the first two size peaks. Here the normalised θ deviation is the amount that the jet angle of a collapse deviates from the mean at that position. 'Normalised' means that the positive sense of normalised θ deviation is always away from the slot. If there were a significant dependence of the jet angle deviation on the jet strength, we would expect to see the spread of normalised jet angle deviation decrease as we increase the normalised displacement. However, both figures do not show any dependence of the jet angle variation on the displacement.

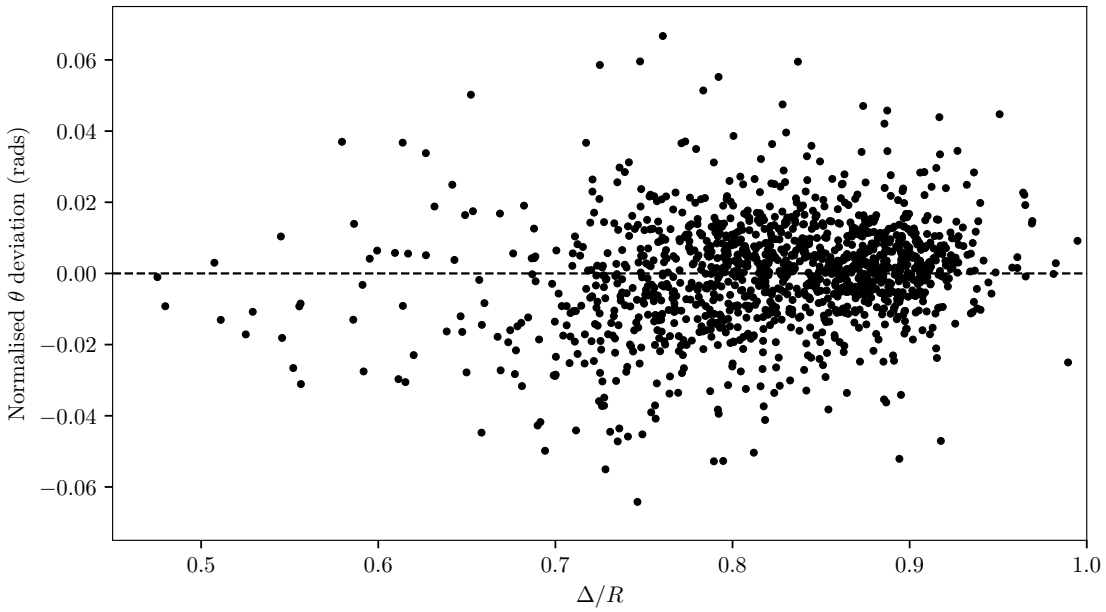

Figure 18: Normalised jet angle deviation as a function of normalised displacement for slot W2H3b with Y = 2.66 mm.

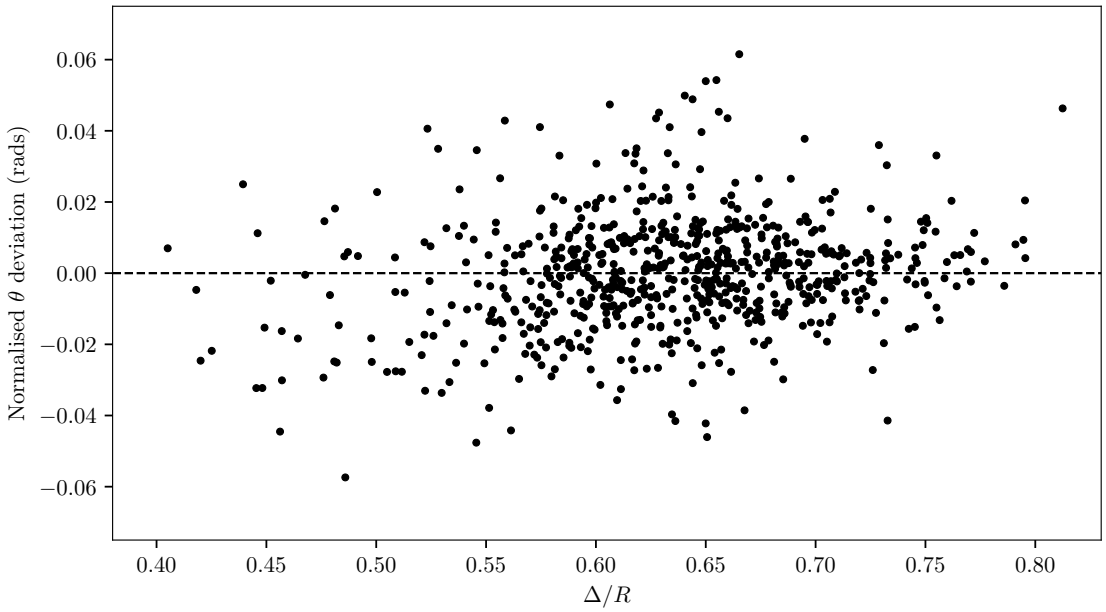

Figure 19: Normalised jet angle deviation as a function of normalised displacement for slot W2H3b with Y = 3.68 mm.